Synthesis and Fluxional Behavior, Including a Comparative Analysis of the Pd−N Bond Rupture, of New Chiral Complexes of Palladium(0) and -(II) with a Rigid (Aminoferrocenyl)phosphine Ligand. Crystal Structure of the Two Rotamers of a Palladium(0) Maleic Anhydride Complex

Felipe Gómez-de la Torre, Félix A. Jalón, Ana López-Agenjo, Blanca R. Manzano,*,† and Ana Rodríguez

Departamento de Química Inorgánica, Orgánica y Bioquímica, Facultad de Químicas, Campus Universitario, 13071 Ciudad Real, Spain

Thomas Sturm and Walter Weissensteiner*,‡

Institut für Organische Chemie, Universität Wien, Währinger Straβe 38, A-1090 Wien, Austria

Martín Martínez-Ripoll

Instituto Rocasolano del CSIC, Serrano,119, 28006 Madrid, Spain

Received April 23, 1998

The (aminoferrocenyl)phosphine ligand 1-diphenylphosphino-2,1′-(1-dimethylaminopropanediyl)ferrocene, **1**, was used to synthesize new palladium(0) and -(II) complexes. The reaction of $Pd_2(dba)_3{\cdot}CHCl_3$ with **1** in the presence of the electron-withdrawing olefins dimethylfumarate (DMFU) and maleic anhydride (MA) gave the new complexes Pd(**1**)(DMFU) (**2**) and Pd(**1**)(MA) (**3**). The allyl complex [Pd(η^3-2-Me-C_3H_4)(**1**)]Tf (**4**) was obtained from the reaction of **1** with [Pd(η^3-2-Me-C_3H_4)(Cl)]$_2$ in the presence of AgTf. In solution all these compounds exist as mixtures of two diastereomers, with either the alkene or the allyl group differently oriented with respect to the aminophosphine ligand. The orientation of these ligands in the major isomers has been determined by means of NOEs. Alkene rotation takes place in complexes **2** and **3** with free energies of activation $\Delta G_{340}^{\ddagger} = 73.1$ kJ mol^{-1} (**2**) and $\Delta G_{368}^{\ddagger} = 79.9$ kJ mol^{-1} (**3**), respectively. These barriers are compared with those of some analogous ferrocenyl aminophosphine ligands, PPFA (2-(1-dimethylaminoethyl)-1-diphenylphosphinoferrocene) and PTFA (1-diphenylphosphino-2,3-*endo*-(α-dimethylamino)tetramethyleneferrocene) complexes. For **3**, the alkene rotation leads to isomer interconversion, while the observed isomerization of **2** must proceed via an olefin face exchange. Some experiments in relation to the nature of this process are discussed. Starting from PdRR′L′ precursors and **1** or PPFA, other Pd(II) derivatives of formulas PdRR′(**1**), R = Cl, R′ = Me, L′ = cod, **5**; R = R′ = Me, L′ = tmeda, **6**; R = R′ = C_6F_5, L′ = cod, **7**, or PdClMe(PPFA), **8**, were prepared. For **5** and **8**, only the isomers with the methyl group trans to nitrogen were obtained. The Pd−N bond rupture in the new complexes of **1** and in similar derivatives of PPFA and PTFA has been analyzed by variable-temperature ^{1}H NMR studies, and in some cases a line shape analysis has been carried out. The influence of the ferrocenyl aminophosphine and ancillary ligands as well as of the oxidation state of the palladium center on this process is discussed. The molecular structures of both rotamers of **3**, present in the same crystal, were determined by X-ray structure analysis.

Introduction

Enantiopure ferrocenyl aminophosphines[1] such as 2-(1-dimethylaminoethyl)-1-diphenylphosphinoferrocene,[2] PPFA (Chart 1), as well as a number of ferrocenyl pyrazol derivatives[3] have been used successfully as P−N coordinating ligands of a variety of homogeneous catalysts. Catalytic reactions include inter alia allylic alkylations, allylic aminations, hydroborations, and Grignard cross-coupling reactions.[4] A typical example of a Grignard cross-coupling is the reaction of vinyl bromide and phenylethylmagnesium chloride giving 3-phenylbutene as the final product. Originally, with use of $PdCl_2$(PPFA) as the catalyst precursor, an enantioselectivity of 68% was obtained.[2d]

† Fax: 34 926 295318. E-mail: bmanzano@qino-cr.uclm.es.
‡ E-mail: Walter.Weissensteiner@univie.ac.at.

(1) Togni, A., Hayashi, T., Eds. *Ferrocenes, Homogeneous Catalysis, Organic Synthesis, Material Science*; VCH: Weinheim, Germany, 1995.

S0276-7333(98)00312-4 CCC: $15.00
Publication on Web 09/19/1998

Chart 1. Configuration of (*S*,*R*)-PPFA, (*R*,*R*)-PTFA, and (*R*,*R*)-1

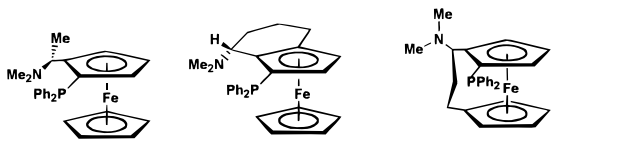

PPFA

PdClMe(PPFA), 8
$PdCl_2$(PPFA), 9

PTFA

1

Pd(1)(DMFU), 2
Pd(1)(MA), 3
[Pd(η^3-2-Me-C_3H_4)(1)]Tf, 4
PdClMe(1), 5
$PdMe_2$(1), 6
$Pd(C_6F_5)_2$(1), 7

We recently reported the synthesis of two new conformationally less flexible ferrocenyl aminophosphines,[5] 1-diphenylphosphino-2,3-*endo*-(α-dimethylamino)tetramethyleneferrocene, PTFA, and 1-diphenylphosphino-2,1′-(1-dimethylaminopropanediyl)ferrocene, **1** (Chart 1), which in the above Grignard cross-coupling reaction gave the product with 79% and 63% ee, respectively. This type of palladium-catalyzed Grignard cross-coupling reaction is thought to proceed via Pd(0) and Pd(II) intermediates, and the enantioselective step is assumed to be the transmetalation step in which the phenylethyl group is transferred from the Grignard reagent onto the palladium catalyst.[6] According to a proposal by Kumada and Hayashi,[2d,7] this step involves a Pd−N bond cleavage of the (PPFA)Pd(vinyl)Br intermediate followed by a coordination of the Grignard reagent to the uncoordinated nitrogen prior to the transfer of the Grignard alkyl group to palladium. Other authors have suggested that the partial dissociation of a chiral ferrocenyl P−N[3a,c] or P−S[8] ligand may be the origin of lower enantioselectivities in some catalytic reactions. Very recently we could show by means of NMR spectroscopy that, indeed, a palladium nitrogen bond cleavage can be observed for PPFA−Pd(0) and PPFA−Pd(II) complexes but not for the respective PTFA derivatives.[9d] Other cases of Pd−N bond rupture have been proposed recently in the literature.[9] Since at least for PPFA complexes the activation barriers of these Pd−N bond rupture processes are rather low and can be observed on the NMR time scale even for the [Pd(η^3-2-Me-C_3H_4)(PPFA)]CF_3SO_3 complex, it is likely that under catalysis conditions such a Pd−N bond cleavage is a fast process not only in Grignard cross-couplings but also in allylic alkylations, allylic amination, or related reactions. Thus, to identify more general trends or correlations, it was of interest to investigate in addition to PPFA and PTFA a broader range of additional ferrocenyl P−N coordinating palladium complexes.

In this paper we describe the synthesis and the fluxional behavior of Pd(0) complexes of ligand **1** with maleic anhydride (MA) and dimethyl fumarate (DMFU) as well as of a number of Pd(II) complexes PdRR′(**1**) (RR′ = 2-methylallyl; R = R′ = C_6F_5; R = R′ = Me; R′ = Me, R = Cl). The set of data obtained for these complexes is compared to those of the related PPFA and PTFA complexes. PdClMe(PPFA) and $PdCl_2$(PPFA)[2d,e] have also been synthesized in order to make complementary NMR studies. Trends in the activation barriers for the different dynamic processes (P−N bond cleavage, olefin rotations, allyl interconversions) are discussed. In addition, the molecular structures of both rotamers of the Pd(**1**)(MA) complex are reported.

Results and Discussion

Synthesis. Palladium(0) complexes were obtained according to eq 1. Reaction of $Pd_2(dba)_3$·$CHCl_3$ (dba = dibenzylideneacetone) in toluene with **1** in the presence of the electron-poor olefin (L) dimethyl fumarate (DMFU) or maleic anhydride (MA) gave the new complexes Pd(**1**)(L).

$$Pd_2(dba)_3\cdot CHCl_3 + 2\mathbf{1} + 2L \rightarrow \underset{\mathbf{2},\ \mathbf{3}}{2Pd(\mathbf{1})(L)} + 3dba \quad (1)$$

L = DMFU, **2**; MA, **3**

The allyl complex [Pd(η^3-2-Me-C_3H_4)(**1**)]Tf (**4**) was synthesized, according to a method described in the literature,[10] by reacting [Pd(η^3-2-Me-C_3H_4)Cl]$_2$ with **1** in the presence of silver triflate (eq 2)

$$[Pd(\eta^3\text{-2-Me-}C_3H_4)Cl]_2 + 2\mathbf{1} + 2AgTf \rightarrow \underset{\mathbf{4}}{2[Pd(\eta^3\text{-2-Me-}C_3H_4)(\mathbf{1})]Tf} + 2AgCl \quad (2)$$

Displacement of weakly coordinated ligands from the corresponding starting materials allows the isolation of new palladium(II) complexes of formula PdRR′(**1**) (see eq 3).

(2) (a) Marquarding, D.; Klusacek, H.; Gokel, G.; Hoffmann, P.; Ugi, I. *J. Am. Chem. Soc.* **1970**, *92*, 5389. (b) Hayashi, T.; Yamamoto, K.; Kumada, M. *Tetrahedron Lett.* **1974**, 4405. (c) Hayashi, T.; Mise, T.; Fukushima, M.; Kagotani, M.; Nagashima, N.; Hamada, Y.; Matsumoto, A.; Kawakami, S.; Konishi, M.; Yamamoto, K.; Kumada, M. *Bull. Chem. Soc. Jpn.* **1980**, *53*, 1138. (d) Hayashi, T.; Konishi, M.; Fukushima, M.; Mise, T.; Kagotani, M.; Tajika, M.; Kumada, M. *J. Am. Chem. Soc.* **1982**, *104*, 180. (e) Hayashi, T.; Konishi; M.; Ito, H.; Kumada, M. *J. Am. Chem. Soc.* **1982**, *104*, 4962. (f) van der Steen, F. H.; Kanters, J. A. *Acta Crystallogr.* **1986**, *C42*, 547.

(3) (a) Schnyder, A.; Hintermann, L.; Togni, A. *Angew. Chem., Int. Ed. Engl.* **1995**, *34*, 931. (b) Togni, A. *Chimia* **1996**, *50*, 86. (c) Schnyder, A.; Togni, A.; Wiesli, U. *Organometallics* **1997**, *16*, 255. (d) Burckhardt, U.; Baumann, M.; Togni, A. *Tetrahedron: Asymmetry* **1997**, *8*, 155. (e) Burckhart, U.; Gramlich, V.; Hofmann, P.; Nesper, R.; Pregosin, P. S.; Salzmann, R.; Togni, A. *Organometallics* **1996**, *15*, 3496. (f) Togni, A.; Burckhart, U.; Gramlich, V.; Pregosin, P. S.; Salzmann, R. *J. Am. Chem. Soc.* **1996**, *118*, 1031. (g) Blöchl, P. E.; Togni, A. *Organometallics* **1996**, *15*, 4125.

(4) (a) Hayashi, T. *Pure Appl. Chem.* **1988**, *60*, 7. (b) Sawamura, M.; Ito, Y. *Chem. Rev.* **1992**, *92*, 857. (c) Brunner, H.; Zettlmeier, W. *Handbook of Enantioselective Catalysis with Transition Metal Compounds*; VCH: Weinheim, Germany, 1993. (d) Ojima, I., Ed.; *Catalytic Asymmetric Synthesis*; VCH: Weinheim, Germany, 1993. (e) Hayashi, T. Asymmetric Catalysis with Chiral Ferrocenylphosphine Ligands. in ref 1, p 105. (f) Togni, A. *Angew. Chem., Int. Ed. Engl.* **1996**, *35*, 1475.

(5) (a) Jedlicka, B.; Widhalm, M.; Weissensteiner, W. *J. Chem. Soc., Chem. Commun.* **1993**, 1329. (b) Mernyi, A.; Kratky, C.; Weissensteiner, W.; Widhalm, M. *J. Organomet. Chem.* **1993**, *370*, 397.

(6) (a) Baker, K. V.; Brown, J. M.; Cooley, N. A.; Hughes, G. D.; Taylor, R. J. *J. Organomet. Chem.* **1993**, *370*, 397. (b) Brown, J. M.; Cooley, N. A. *Chem. Rev.* **1988**, *88*, 1031. (c) Indolese, A.; Consiglio, G. *J. Organomet. Chem.* **1993**, *463*, 209.

(7) Hayashi, T.; Kumada, M. *Acc. Chem. Res.* **1982**, *15*, 395.

(8) Albinati, A.; Eckert, J.; Pregosin, P.; Rüegger, H.; Salzmann, R.; Stössel, C. *Organometallics* **1997**, *16*, 579.

(9) (a) Albinati, A.; Kunz, R. W.; Ammann, C. J.; Pregosin, P. S. *Organometallics* **1991**, *10*, 1800. (b) Gogoll, A.; Örnebro, J.; Grennberg, H.; Bäckvall, J.-E. *J. Am. Chem. Soc.* **1994**, *116*, 3631. (c) Elguero, J.; Fruchier, A.; de la Hoz, A.; Jalón, F. A.; Manzano, B. R.; Otero, A.; Gómez-de la Torre, F. *Chem. Ber.* **1996**, *129*, 589. (d) Fernández-Galán, R.; Jalón, F. A.; Manzano, B. R.; Rodríguez-de la Fuente, J.; Vrahami, M.; Jedlicka, B.; Weissensteiner, W.; Jogl, G. *Organometallics* **1997**, *16*, 3758. (e) Gogoll, A.; Grennberg, H.; Axén, A. *Organometallics* **1997**, *16*, 1167.

(10) Breutel, C.; Pregosin, P. S.; Salzmann, R.; Togni, A. *J. Am. Chem. Soc.* **1994**, *116*, 4067.

$$PdRR'(L') + \mathbf{1} \rightarrow PdRR'(\mathbf{1}) + L' \qquad (3)$$
$$\mathbf{5-7}$$

R = Cl, R′ = Me, L′ = 1,5-cyclooctadiene (COD), **5**; R = R′ = Me, L′ = tetramethylethylenediamine (TMEDA), **6**; R = R′ = C_6F_5 , L′ = COD, **7**.

Using the same method, the derivatives PdClMe(PPFA), **8** (from PdClMe(COD)), and $PdCl_2$(PPFA),[2d,e] **9** (from $PdCl_2(PhCN)_2$), have also been prepared.

All complexes are soluble in the polar solvents acetone or chloroform and, except **4**, are also soluble in toluene or benzene. They are highly stable in the solid state if stored under nitrogen. In solution, the Pd(0) complexes as well as **6** slowly decompose. In halogenated solvents, **6** evolves quickly and quantitatively to **5**, which in a slow transformation reacts further, giving $PdCl_2$(**1**) as the final product. All other complexes are stable in solution.

NMR Characterization of the New Palladium Complexes. Complexes **2**−**4** exist in solution always as a mixture of two diastereomers (major, M, and minor, m) (see Chart 2) whose ratio, which usually depends on the solvent nature, was deduced from the ^{1}H NMR spectra at room temperature and is indicated in Table 1. Those isomers differ in how either the alkene or the allyl group is oriented with respect to the amino phosphine ligand. For related ferrocenyl phosphine palladium derivatives, such a mixture of diastereomers has been observed previously by us[9d,11] and others.[3e,f,8,12] Although in some N,P-ferrocenyl palladium complexes[3e] conformational isomers involving the chelate ring have been observed by ^{1}H NMR at low temperature, this fact is not frequent, and for complexes of **1,** the possibility of such conformational isomers can be ruled out. This is due to the fact that, although two conformations are possible[5b] for noncoordinated **1** (see Chart 3), only the conformation a, which according to previous calculations is 22 kJ mol^{-1} more stable than conformation b, is suitable for a chelate coordination. In this orientation the heteroannular chain has the central carbon pointing toward the phosphorus atom, and as a consequence, the NMe_2 group is located above Cp^1.

In Tables 1−3, ^{1}H and ^{13}C NMR chemical shifts as well as coupling constants are given for selected signals of the aminophosphine and ancillary ligands of complexes **2**−**8**. For complexes **5**, **6**, and **8**, the methyl resonances are indicated in the Experimental Section. The rest of the data are given as Supporting Information. On complexation of the aminophosphine ligands, some general trends are observed for the resonances of all these derivatives: (i) the two equivalent amino methyl groups of **1** or PPFA are deshielded and transformed into two diastereotopic singlets in both ^{1}H and ^{13}C NMR spectra, (ii) as compared to **1** or PPFA, the ^{31}P NMR resonances are shifted downfield by 27−49 ppm, and (iii) in cases of complexes with **1**, the P-coordination and the special rigidity of this ferrocenyl ligand lead to a particular orientation of one of the phenyl groups that shields the H(5′) proton (δ = 2−3 ppm) of Cp^2 (see Chart 3, conformation a).

Chart 2. Observed Diastereomers of 2-4[a]

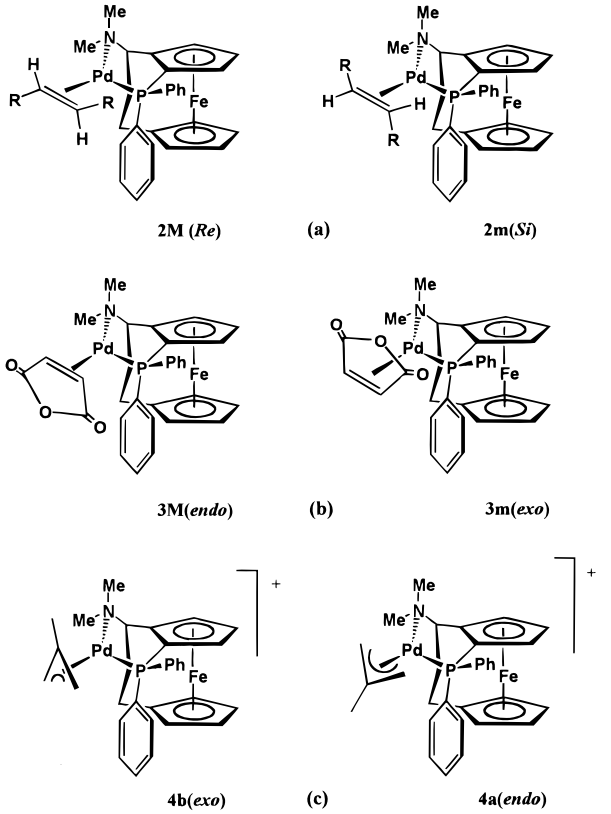

[a] R = CO_2Me. Conformation of different isomers has been elucidated by NOE studies (see text and Chart 4). *Re* and *Si* refer to the olefin face coordinated to the Pd center, and *endo* and *exo* refer to the orientation of the endocyclic oxygen of the MA or the allyl group pointing toward or away from the ferrocene core.

The proton resonances of the two diastereomers mixtures of derivatives **2**−**4** were assigned mainly with the use of COSY spectra. This allowed us not only to classify the seven Cp signals of each isomer but also to differentiate the resonances corresponding to the Cp^1 and Cp^2 rings. This has not been possible for **4**, which shows a quite similar ratio of isomers and too many overlapping signals. Except for **4**, the protons of the trimethylene bridges have also been completely assigned, mainly on the basis of COSY experiments and the analysis of the spin systems. In all cases, where the coupling constants of the chain proton attached to carbon 1c (for the numbering scheme, see Chart 3) could be analyzed, the chain conformation with the dimethylamino group pointing straight above Cp^1 is found. (By analogy, these resonances have also been assigned for complexes **5**−**7**.) As in the more stable conformation of the free ligand,[5b] in complexes **2**−**4** the central chain carbon, C(2c), is always positioned in close proximity to the phosphorus, which is reflected in the ^{13}C spectra, in which C(2c) is the only chain carbon showing a ^{31}P−^{13}C coupling constant.

The alkene protons and carbons (see Table 2) of the MA and DMFU groups give rise to two separated signals shifted to lower frequency with respect to the free olefins.[13] These shifts, higher for the MA derivative, are in the range usually expected for other zerovalent ML_2(alkene) complexes of palladium and platinum.[14] In

(11) Jedlicka, B.; Rülke, R. E.; Weissensteiner, W.; Fernández-Galán, R.; Jalón, F. A.; Manzano, B. R.; Rodríguez-de la Fuente, J.; Veldman, N.; Koijman, H.; Spek, A. L. *J. Organomet. Chem.* **1996**, *508*, 69.

Table 1. ^{1}H and ^{13}C NMR Data for Ligand 1 in Complexes 2−7 and PPFA in 8[a]

		^{1}H NMR				^{13}C NMR			
						chain			
complex	amt,[b] %	$H_5'(Cp^2)$	$N(CH_3)_2$	*ortho*-Ph_{up}	*ortho*-Ph_{down}	C_1	C_2	C_3	$N(CH_3)_2$
2M	60	2.86(m)	D-2.81(s)	7.40(pt)	8.20(ddd)	69.11	42.57(d)	24.90	*c*
			U-2.19(s)	J = 7.5	J = 11.0, 8.1, 1.5		J = 4.5		
2m	40	2.53(m)	D-2.90(s)	7.27(pt)	7.90(ddd),	68.86	42.87(d)	24.98	*c*
			U-2.25(s)	J = 7.2	J = 10.5, 8.5, 1.5		J = 5.0		
3M	77	3.0(m)	D-2.73(s)	7.26(dd)	7.90(ddd)	68.66	42.18(d)	24.47	51.02
			U-1.99(s)	J = 7.5, 1.5	J = 11.5, 6.9, 1.4		J = 5.0		54.44
3m	23	2.97(m)	D-2.78(s)	7.29(ptd)	7.80(m)	68.77	42.12(d)	24.55	50.62
			U-2.07)s)	J = 9.1, 2.0			J = 5.6		54.21
4a	54	*c*	D-3.29(s)	7.24(m)	8.18(m)	68.82	42.67(d)	24.30	52.52
			U-2.67(s)				J = 5.1		57.18
4b	46	*c*	D-3.28(s)	7.20(m)	7.97(dd)	69.04	42.49	24.13	55.51
			U-2.74(s)		J = 12.2, 7.6		J = 4.0		51.42
5		2.05(m)	D-2.98(s)	7.19(m)	8.11(m)	68.24	41.89(d)	24.70	52.35
			U-2.60(s)				J = 3.0		49.61
6		2.05(m)	D-2.47(s)	7.26(m)	8.13(m)	67.99	42.16(d)	24.94	51.85
			U-2.29(s)				J = 5.0		49.84
7		2.52(m)	D-2.23(s)	6.84(m)	8.1(ddd)	68.74	42.36(d)	24.57	54.78
			U-1.84(s)		J = 11.4, 8.0, 1.7				50.47
8		C*H*Me CH*Me*	D-3.23(s)	7.35(pt)	8.04(m)		*C*HMe CH*Me*		42.68
			U-2.52(s)	J = 11.0					48.59
		3.38(c) 1.04(d) J_{HH} = 6.6					73.47 15.87		

[a] ^{1}H NMR recorded at room temperature in toluene-d_8, (**2**, **8**), benzene-d_6 (**3**, **6**, **7**), chloroform-*d* (**5**), or 1,1,2,2-tetrachloroethane-d_2 (**4**). ^{13}C NMR recorded at room temperature in acetone-d_6 (**2**), chloroform-*d* (**3**−**5**), benzene-d_6 (**6**, **7**), or toluene-d_8 (**8**). The ^{1}H and ^{13}C NMR data of the Cp groups (except the H_5' of complexes with ligand **1**), the ^{13}C NMR signals of the Ph rings and a complete assignment of the ^{1}H NMR resonances of the trimethylene bridge protons are given as Supporting Information. pt = pseudotriplet; M = major isomer; m = minor isomer; D = down; U = up. Up and down refer to the phenyl or Me groups oriented away from or toward the ferrocenyl unit, respectively. For the adopted numbering scheme, see Chart 3. [b] Percentage of the isomers. [c] Signals not clearly distinguished.

Chart 3. Preferred (a) and Less Stable (b) Conformation of ligand 1 and Numbering Scheme of 1 (a)

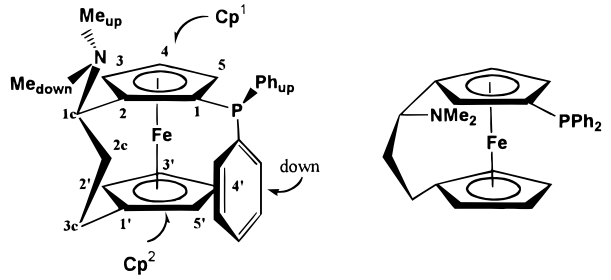

(a) (b)

the case of the ^{1}H NMR signals additional INDOR experiments were carried out. Complex **4** shows four different allyl protons and two terminal allyl carbons for each isomer, reflecting the asymmetric environment in its coordination sphere (see Table 3). The assignment is based on COSY experiments and on characteristic chemical shifts[15] and coupling constants. As expected, the proton and carbon resonances trans to phosphorus appear at higher frequencies according to the stronger trans influence of this atom. A NOE has been found from the allyl methyl to the syn protons, confirming this assignment. As expected,[11] in the case of complex **5**, according to the small coupling constant J_{HP} and J_{CP}[16] observed (see the Experimental Section), only the isomer with the methyl group trans to nitrogen is present.

The structural analysis of the two nonequivalent pentafluorophenyl groups of **7** has been carried out by ^{19}F NMR (see the Experimental Section). The more relevant conclusion is that 10 unique fluorine signals are observed, implying a restricted rotation of the pentafluorophenyl groups around the Pd−C_{ipso} bond, which must be a consequence of the steric requirements of ligand **1**. This fact has been previously observed in other cis palladium and platinum complexes,[17] but usually freely rotating groups are seen.[18]

Stereochemical Assignments of Complexes 2−4. Considering the importance of the particular arrangement of the ligands around the metal center, especially in enantioselective homogeneous catalysis, we have undertaken several NOE studies in order to establish the orientation of the alkene and allyl ligands of the isomers of complexes **2**−**4**. For the equilibrium mixtures of **3** (chloroform-*d* solution, **3M**/**3m** = 62:38) and **4** (acetone-d_6, **4a**/**4b** = 27:73) spectra were recorded at

(12) Pregosin, P. S.; Salzmann, R.; Togni, A. *Organometallics* **1995**, *14*, 842.

(13) ^{1}H (^{13}C) NMR data for the free alkenes in $CDCl_3$: MA, 7.04 (137.1) ppm; DMFU, 6.86 (133.9) ppm.

(14) See, for example: (a) Cenini, S.; Ugo, R.; La Monica, G. *J. Chem. Soc. A* **1971,** 409. (b) Otsuka, S.; Yoshida, T.; Tatsuno, Y. *J. Am. Chem. Soc.* **1971,** *93*, 6462. (c) Ito, T.; Hasegawa, S.; Takahashi, Y.; Ishii, Y. *J. Organomet. Chem.* **1974,** *73*, 401. (d) Ittel, S. D. *Inorg. Chem.* **1977,** *16*, 2589. (e) Itoh, K.; Ueda, F.; Hirai, K.; Ishii, Y. *Chem. Lett.* **1977,** 877. (f) Chicote, M. T.; Green, M.; Spencer, J. L.; Stone, F. G. A.; Vicente, J. *J. Chem. Soc., Dalton Trans.* **1979,** 536. (g) Cavell, K. J.; Stufkens, D. J.; Vrieze, K. *Inorg. Chim. Acta* **1980,** *47*, 67. (h) Krause, J.; Bonrath, W.; Pörschke, K. R. *Organometallics* **1992**, *11*, 1158. (i) van Asselt, R.; Elsevier, C. J.; Smeets, W. J. J.; Spek, A. L. *Inorg. Chem.* **1994**, *33*, 1521. (j) Tschoerner, M.; Trabesinger, G.; Albinati, A.; Pregosin, P. S. *Organometallics* **1997**, *16*, 3447.

(15) Wilkinson, G., Stone, F. G. A., Abel, E. W., Eds. *Comprehensive Organometallic Chemistry*; Pergamon Press: Oxford, U.K., 1982; Vol, 6, p 409.

(16) Baker, K. V.; Brown, J. M.; Cooley, N. A.; Hughes, G. D.; Taylor, R. J. *J. Organomet. Chem.* **1989**, *370*, 397.

(17) See, for example: (a) Casas, J. M.; Forniés, J.; Martín, A.; Menjón, B.; Tomás, M. *J. Chem. Soc., Dalton Trans.* **1995**, 2949. (b) Forniés, J.; Martínez, F.; Navarro, R.; Urriolabeitia, E.; Welch, A. J. *J. Chem. Soc., Dalton Trans.* **1995**, 2805. (c) Ara, I.; Delgado, E.; Forniés, J.; Hernández, E.; Lalinde, E.; Mansilla, N.; Moreno, M. T. *J. Chem. Soc., Dalton Trans.* **1996**, 3201.

Table 2. ^{1}H and ^{13}C NMR Data for the Alkene Ligands in Complexes Pd(1)(alkene) (2, 3)[a]

	^{1}H NMR			^{13}C NMR					
	olef H			olef C		CO		CO_2Me	
complex	cis P	trans P	CO_2Me	cis P	trans P	cis P	trans P	cis P	trans P
2M	4.89(dd)	4.11(pt)	3.57	*b*	48.22(d)	172.97(d)	173.122(d)	*b*	50.24(d)
	$J_{H-P} = 2.6$	$J_{H-P} = 9.6$	2.86		$J = 28.7$	$J \sim 2.3$	$J = 5.5$		$J = 15.6$
	$J_{H-H} = 9.7$	$J_{H-H} = 9.7$							
2m	4.16(*ABX*)	4.16(*ABX*)	3.41	*b*	49.56(d)	174.51(d)	172.72(d)	*b*	50.33(d)
	$J_{H-P} = 2.9$	$J_{H-P} = 10.5$	3.34		$J = 29.2$	$J \sim 2.3$	$J = 5.6$		$J = 20.7$
	$J_{H-H} = 9.8$	$J_{H-H} = 9.8$							
3M	3.91(pt)	3.45(dd)		47.64(d)	48.35(d)	172.82(s)	170.93(d)		
	$J_{H-P} = 3.7$	$J_{H-P} = 10.0$		$J = 2.21$	$J = 29.7$		$J = 5.0$		
	$J_{H-H} = 3.9$	$J_{H-H} = 3.9$							
3m	4.31(pt)	3.66		47.43(s)	48.35(d)	170.90(s)	171.35(d)		
	$J_{H-P} = 3.4$				$J = 29.7$		$J = 5.1$		
	$J_{H-H} = 3.4$								

[a] Spectra recorded at room temperature. ^{1}H NMR in toluene-d_8 (**2**) or benzene-d_6 (**3**). ^{13}C NMR in acetone-d_6 (**2**) or chloroform-*d* (**3**). M = major isomer; m = minor isomer. [b] Signals not clearly distinguished.

Table 3. ^{1}H and ^{13}C NMR Data for the Allyl Group in [Pd(2-Me-C_3H_4)(1)]Tf (4)[a]

						^{13}C			
	^{1}H NMR					CH_2			
complex	Me	H_s cis P	H_a cis P	H_s trans P	H_a trans P	cis P	trans P	Me	−C=
4a	2.25(s)	2.89(bs)	2.75(bs)	4.35(m)	3.65(d)	57.49(s)	80.32(d)	22.91(s)	*b*
					$J = 9.3$		$J = 30.2$		
4b	1.38(s)	3.50(bs)	1.92(bs)	4.45(m)	3.59(d)	59.02(s)	82.04(d)	23.57(s)	*b*
					$J = 11.0$		$J = 28.7$		

[a] ^{1}H NMR (1,1,2,2,-tetrachloroethane-d_2) and ^{13}C NMR (chloroform-*d*) spectra recorded at room temperature. M = major isomer; m = minor isomer. s = syn; a = anti. [b] Signals not clearly distinguished; they appear in the phenylic region.

233 K in order to slow the isomer interconversion (see Fluxional Behavior section). In the case of complex **2** (benzene-d_6), a sample with only the major isomer, obtained from crystallization of the isomer mixture, was measured.

In all these complexes, the cyclopentadienyl protons H(5′) (see Chart 3) are in close proximity to the phenyl ring pointing toward Cp[2] allowing the measurement of an NOE from H(5′) to the ortho phenyl protons (ortho-Ph_{down}). A clear but less intense NOE is observed between one of the amino methyl groups and one Cp[1] proton. Taking into account the rigidity of **1** when coordinated, these resonances can be assigned to the amino methyl pointing toward the distal Cp[1] side (Me_{up}) and the Cp[1] proton H(3), respectively. An NOE has also been observed from this Me_{up} to the ortho protons of the adjacent phenyl group (Ph_{up}). These data show that for each complex **2**−**4** the signals for both the Me_{up} and the ortho-Ph_{up} appear always at higher field than the corresponding groups situated down (Table 1). The corresponding signals of **5**−**7** have been assigned by analogy.

In Chart 4, the observed NOEs for complexes **2M**, **3M**, and both isomers of **4**, which have allowed their stereochemical assignment, are indicated by arrows. Several NOEs have been found between the Me_{up} and the ortho-Ph_{up} hydrogens and different olefinic protons or the allylic methyl group situated above the Pd coordination plane (**2M**, **3M**, and **4b**). In **2M** and **4a**, NOEs between the ortho-Ph_{down} protons and the respective groups situated below this plane are observed.

Chart 4. Main NOEs Observed for Complexes 2M, 3M, 4a, and 4b

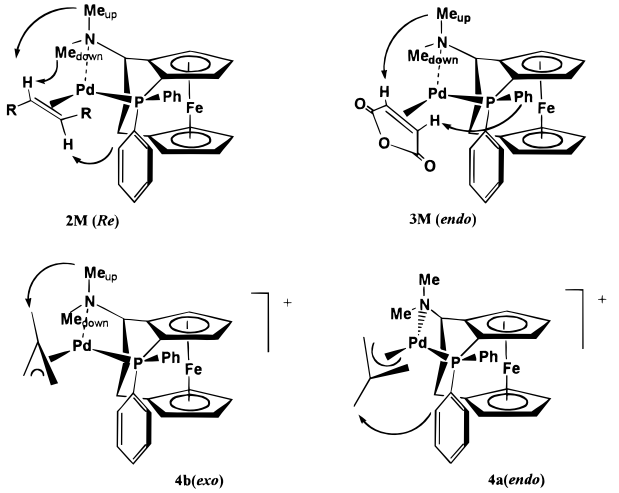

Fluxional Behavior of Complexes 2−8. We have carried out variable-temperature ^{1}H NMR studies for complexes **2**−**8** (**2**, **3**, **5**−**8** in toluene-d_8 and **4** in 1,1,2,2-tetrachloroethane-d_2) over the full temperature range of the solvents. The different dynamic processes expected to be present in this type of complexes can be divided into two groups: isomer interconversion and Pd−N bond rupture processes. According to our previous results for ferrocenyl aminophosphine palladium complexes,[9d] this bond rupture is a feasible process, while the cleavage of the stronger Pd−P bond is rather unlikely.

(18) See for example: (a) Usón, R.; Forniés, J.; Espinet, P.; Fortuño, C.; Tomás, M. *J. Chem. Soc., Dalton Trans.* **1988**, 3005. (b) Usón, R.; Forniés, J.; Tomás, M.; Menjón, B.; Fortuño, C.; Welch, A. J.; Smith, D. E.. *J. Chem. Soc., Dalton Trans.* **1993**, 275. (c) Casas, J. M.; Falvello, L. R.; Forniés, J.; Martín, A.; Tomás, M. *J. Chem. Soc., Dalton Trans.* **1993**, 1107. (d) Usón, R.; Forniés, J.; Usón, M. A.; Tomás, M.; Ibañez, M. A. *J. Chem. Soc., Dalton Trans.* **1994**, 401. (e) Ara, I.; Forniés, J.; Lalinde, E.; Moreno, M. T.; Tomás, M.. *J. Chem. Soc., Dalton Trans.* **1994**, 2735. (f) Falvello, L. R.; Forniés, J.; Navarro, R.; Sicilia, V.; Tomás, M. *J. Chem. Soc., Dalton Trans.* **1994**, 3143. (g) Forniés, J.; Lalinde, E.; Martín, A.; Moreno, M. T.; Welch, A. J. *J. Chem. Soc., Dalton Trans.* **1995**, 1333.

Table 4. Free Activation Energies Related with Alkene Rotation for PdFec(MA) and PdFec(DMFU) (Fec = PPFA, PTFA, 1) Complexes

entry no.	complex	$\delta\nu$ (Hz)	T_c (K)	$\Delta G_c^{\ddagger a}$ (kJ/mol)	interchanging groups	ref
1	Pd(**1**)(DMFU), **2**	2.9	320	67.9	alkene protons (m)	*b*
2	**2**	18.75	340	73.1	alkene methyls (m)	*b*
3	Pd(PTFA)(DMFU), **10**	52.7	330	68.0	alkene methyls (m)	9d
4	**10**	168.2	353	69.5	alkene protons (m)	9d
5	**10**	114.0	358	71.7	alkene methyls (M)	9d
6	**10**	250.0	373	72.4	alkene protons (M)	9d
7	Pd(PPFA)(DMFU), **11**	250.0	298	57.3	alkene protons (M)	9d
8	Pd(**1**)(MA), **3**	16.04	368	80.0 (83.7)	aminomethyls (up) (M+m)	*b*
9	**3**	16.70	368	79.9 (83.6)	aminomethyls (down) (M+m)	*b*
10	Pd(PTFA)(MA), **12**	10.2	338	74.6 (76.5)	aminomethyls (up) (M+m)	9d
11	**12**	18.3	346	74.8 (76.7)	aminomethyls (down) (M+m)	9d
12	Pd(PPFA)(MA), **13**	11.0	293	64.1 (66.5)	aminomethyls (up) (M+m)	9d
13	**13**	16.4	303	65.4 (67.9)	aminomethyls (down) (M+m)	9d
14	**13**	32.0	313	65.9 (68.5)	alkene protons (M+m)	9d

[a] See Experimental Section for the calculation method used. [b] This paper. For complexes **3**, **12**, and **13**, minor (m) to major (M) (major to minor) isomer transformations are given.

Table 5. Free Activation Energies Related with Isomer Interconversion for [Pd(2-Me-allyl)Fec]Tf (Fec = PPFA, PTFA, 1)

entry	complex	$\delta\nu$ (Hz)	T_c (K)	$\Delta G_c^{\ddagger a}$ (kJ/mol)	interchanging groups	ref
1	[Pd(2-Me-allyl)(**1**)]Tf, **4**	5.5	355	80.3 (80.8)	aminomethyls (down) (M+m)	*b*
2	**4**	28.5	385	82.1 (82.6)	aminomethyls (up) (M+m)	*b*
3	[Pd(2-Me-allyl)(PPFA)]Tf, **14**	6.6	345	77.4 (77.9)	nonfunctionalized Cp (M+m)	9d
4	[Pd(2-Me-allyl)(PTFA)]Tf, **15**	21.5	351	75.4 (76.0)	$H_{syn,trans}$(M) ↔ $H_{syn,trans}$(m)	9d
5	**15**	37.4	359	75.6 (76.2)	nonfunctionalized Cp (M+m)	9d
6	**15**	42.4	361	75.6 (76.2)	aminomethyls (M+m)	9d

[a] See Experimental Section for the calculation method used. [b] This paper. Minor (m) to major (M) (major to minor) isomer transformations are given.

Isomer Interconversion for 2−4. In our studies, several coalescences related to olefin rotation or/and diastereomer interconversion have been observed, and the corresponding data of coalescence temperature and free energy of activation at this temperature are listed in Tables 4 and 5. In case of the olefin complex **3**, a simple rotation leads to isomer interconversion (alkene symmetry: C_{2v}), whereas for the DMFU derivative, **2** (alkene symmetry: C_{2h}), the rotation gives rise only to an interchange of the olefin substituents; however, in order to achieve an isomer interconversion, a process that exchanges the olefin faces must be operating (see Chart 2). For this complex, a coalescence of the two ester methyl resonances of the minor isomer is observed. Also the AB system (^{31}P-decoupled) of the alkene protons of this isomer (**2m)** transforms into an A_2 system, whose singlet narrows with increasing temperature. The corresponding alkene signals of **2M** broaden enormously, but the higher chemical shift difference $\delta\nu$ prevents the coalescence to be clearly observed up to the maximum temperature registered (378 K). All these observations are in agreement with an alkene rotation process. The $\Delta G^{\ddagger}$ values are in accordance with values reported in the literature for alkene rotation of different types of complexes,[19] especially for those of the closely related Pd(L−L)(alkene), L−L = PPFA, PTFA,[9d] and diimine.[14i] However, some Pd(0) examples where the olefin rotation could not be observed have been described.[14h] For theoretical studies about alkene rotation see, for example, ref 20. No coalescence phenomenon corresponding to an isomer interconversion **2M** ⇔ **2m** could be detected up to the maximum temperature recorded. To calculate the barrier of the possible isomerization process **2M** ⇔ **2m**, we have monitored the transformation of isolated **2M** into **2m** by ^{1}H NMR in benzene-d_6 at 40 °C until an equilibrium ratio was reached (6:4 ratio, 6 h). A barrier of $\Delta G^{\ddagger}_{313} = 110$ kJ mol^{-1} was calculated.

With the aim of obtaining information about the isomerization mechanism, several additional ^{1}H NMR experiments (in benzene-d_6 at 40 °C) have been carried out:[21] (i) When a small amount of free DMFU (0.2 equiv) is added, the barrier of the isomerization decreases to 103.5 kJ mol^{-1} at 40 °C. In the presence of free alkene, this acceleration effect suggest an associative rather than a dissociative mechanism. (ii) To demonstrate that for **2M** an inter- rather than an intramolecular olefin interchange takes place, 1 equiv of free *trans*-CD_3CO_2−CH=CH−CO_2CD_3 (DMFU-d_6) was added to a solution of **2M** in benzene-d_6 at 40 °C. **2M** was transformed into a mixture of **2M** and **2m** as well as into the deuterated complexes. The isomerization process **2M** ⇔ **2m** and the alkene substitution are observed simultaneously with identical barriers ($\Delta G^{\ddagger}_{313}$ = 102.6 and 102.1 kJ mol^{-1}, respectively). Experiments i and ii have been performed in the presence of free alkene, which may open up the possibility of associative mechanisms. To determine whether a spontaneous olefin dissociation takes place in the absence of free ligand, a third experiment has been carried out: (iii) An equimolar mixture of **2M** and Pd(PPFA)(DMFU-d_6) was prepared and studied by ^{1}H NMR. The ester methyl signals of Pd(PPFA)(DMFU) appeared; hence, an interchange of the alkene ligands between the Pd(NP) fragments must have taken place. A similar interchange has been

(19) Ref 15, Vol. 3, pp 103−109.

(20) (a) Wheebock, K. S.; Nelson, J. H.; Cusachs, L. C.; Jonassen, H. B. *J. Am. Chem. Soc.* **1970**, *92*, 5110. (b) Albright, T. A.; Hoffmann, R.; Thibeault, J. C.; Thorn, D. L. *J. Am. Chem. Soc.* **1979**, *101*, 3801.

(21) The noncoordinating character of this solvent makes its participation in the process less likely.

described by Elsevier[14i] for Pd(diimine)(alkene) complexes. Simultaneously to the olefin exchange, also the **2M** ⇔ **2m** isomerization occurs. Both alkene cross-interchange and isomerization show nearly identical free energies of activation: $\Delta G^{\ddagger}_{313} = 107.3$ and 106.0 kJ mol^{-1}, respectively. This points to a common limiting rate-determining step in both processes, with the olefin dissociation being the most reasonable alternative. Although the differences are not very pronounced, the isomerization barriers found in experiment iii are between those observed for pure **2M** and **2M** in the presence of free DMFU. This may be due to the fact that the Pd(PPFA)(DMFU) complex dissociates the olefin more easily than **2**, which parallels the observation of smaller olefin rotation barriers in PPFA complexes as compared to complexes of **1**. See below for a more general discussion of rotational barriers.

The variable-temperature ^{1}H NMR study of complex **3** shows an exchange of the two NMe_{up} signals belonging to unlike isomers, and the same is observed for the two NMe_{down} signals. This evidences unambiguously a **3M** ⇔ **3m** isomer interconversion. In principle, several processes may account for such an observation. Unfortunately, the alkene resonances do not give supplementary information. The four signals of the two isomers broaden and nearly disappear at 378 K, but a coalescence is not clearly reached. Nevertheless, considering our observations for the DMFU complex, **2**, and for other related amino ferrocenyl complexes,[9d] we propose the alkene rotation to be the process causing the observed isomer interconversion.

A comparison of the activation barriers of the alkene rotation in **2** and **3** with those of the corresponding values of the analogous PPFA and PTFA complexes[9d] (see Table 4) shows an order of these barriers of **1** > PTFA > PPFA, both for the DMFU and MA complexes (see ref 22 for arguments). According to these results and from an electronic point of view, it seems that the donor ability of the fragments (Fec)Pd (Fec = ferrocenyl aminophosphine ligands) follows the order **1** > PTFA > PPFA. Although steric effects cannot be fully excluded, a severe steric hindrance of the alkene rotation is very unlikely, as deduced from different X-ray structures of these type of complexes (see refs 9d, 11 and the structure described below).

The data of Table 4 also show that for each aminophosphine ligand the olefin rotation barrier is higher in the MA complexes than in the respective DMFU derivatives, implying a smaller withdrawing character for the latter ligand in these type of complexes (see ref 23 for arguments). In addition, we have observed that complex **2M** is quantitatively transformed into **3** when **2M** is reacted with 1 equiv of MA at 8 °C. This confirms the higher thermodynamic stability of **3** as a consequence of a stronger Pd−alkene bond.

For complex **4**, an isomer interconversion is also indicated by the coalescence of the respective resonances of the NMe_{up} and the NMe_{down} groups (see Table 5). Although the two allylic methyl signals broaden enormously, the high chemical shift difference ($\delta\nu$ about 260 Hz) precludes the observation of the corresponding coalescence below 413 K. In principle, several mechanisms might be proposed to explain the observed isomerization.[24] An $\eta^3-\eta^1-\eta^3$ mechanism is commonly accepted for palladium allyl complexes with ferrocenyl phosphine ligands containing additional P-[10,12,25] or S-[26]-functionalities. Recently, we have shown[9d] that this mechanism is also operating in [Pd(η^3-2-Me-C_3H_4)(PTFA)]Tf, a complex closely related to **4**. Considering these data, an $\eta^3-\eta^1-\eta^3$ pathway is likely to account for the observed isomer interconversion in **4**.

The $\Delta G^{\ddagger}_c$ values for **4** and also for the corresponding allyl complexes with PPFA and PTFA[9d] are summarized in Table 5. These values are higher than those of the corresponding alkene rotations. In this series, the energy increases in the order **1** > PPFA > PTFA (see ref 27 for arguments).

Pd−N Bond Rupture. According to our previous study,[9d] it is possible to observe and investigate Pd−N bond rupture processes in ferrocenyl aminophosphine palladium derivatives on the NMR time scale. We have now studied the influence of different factors such as the nature of the ferrocenyl and ancillary ligands or the oxidation state of the palladium center on the activation parameters of the Pd−N bond cleavage. If the energy barrier involved in the Pd−N bond rupture is low enough, a broadening and in some cases also a coalescence of the two diastereotopic aminomethyl groups of a specific complex are observed. The chemical interchange between these two groups requires, after the Pd−N bond rupture and prior to the recoordination to the unsaturated metal center, an inversion at the nitrogen atom and a rotation of the whole dimethylamino group. It is reasonable to assume that from all these consecutive steps the Pd−N bond cleavage contributes most to the measured activation barrier. In neither case of complexes **2**−**7**, all derivatives of ligand **1**, could a signal coalescence be reached up to the maximum temperature registered. For complex **6**, a marked broadening of the aminomethyl signals is observed, but, due to the product decomposition which is completed at about 353 K, a proper analysis of the line width evolution and the detection of the coalescence temperature were not possible. Only a slight broadening of the aminomethyl resonances was observed at high

(22) To establish this order we have taken into account the $\Delta G^{\ddagger}_c$, T_c, and $\delta\nu$ values, considering especially that $\Delta G^{\ddagger}_c$ changes with temperature. Table 4 shows, for example, that for the DMFU derivatives the T_c value (340 K) given in entry 2 lies between the two T_c values of entries 3 and 4, but $\Delta G^{\ddagger}_c$ is higher for the complex with ligand **1** (**2**), (**1** > PTFA). On the other hand, in entries 6 and 7, the $\delta\nu$'s are equal but the T_c and also the $\Delta G^{\ddagger}_c$ values are clearly higher for the complex with PTFA (**10**) (PTFA > PPFA). In the case of MA complexes, the $\delta\nu$ is higher in entry 11 than in 8, but the inverse order is found for the T_c and $\Delta G^{\ddagger}_c$ values (**1** > PTFA). The same comparison can be made with entries 10 and 14 to compare PPFA and PTFA complexes, (PTFA > PPFA).

(23) A comparison of the two complexes with ligand **1** (Table 4) shows that although in entry 2 the $\delta\nu$ is higher than in entry 8, the T_c and also $\Delta G^{\ddagger}_c$ values are smaller for entry 2 (DMFU derivative). For the PTFA complexes, the T_c values of entries 10 and 11 are between those of entries 3 and 4, while the $\Delta G^{\ddagger}_c$ data are clearly higher in 10 and 11 (MA complex). A similar comparison can be made for the PPFA derivatives. The T_c of entry 7 (298 K) is between the T_c values of entries 12 and 13, and the $\Delta G^{\ddagger}_c$ for the DMFU complex is notably smaller.

(24) Vrieze, K. In *Dynamic Nuclear Magnetic Resonance Spectroscopy;* Jackman, L. M., Cotton, F. A., Eds.; Academic Press: NewYork, 1975.

(25) Pregosin, P. S.; Salzmann, R. *Coord. Chem. Rev.* **1996**, *155*, 35.

(26) Herrmann, J.; Pregosin, P. S.; Salzmann, R.; Albinati, A. *Organometallics* **1995**, *14*, 3311.

(27) The difference between PPFA and **1** is not very pronounced. A comparison of entries 1 and 3 shows that the smaller $\delta\nu$ corresponds to the higher T_c and $\Delta G^{\ddagger}_c$ (complex **4**). The comparison between the PPFA and PTFA derivatives can be made with use of entries 3 and 4. For a lower T_c, a higher $\Delta G^{\ddagger}_c$ is observed for the PPFA complex.

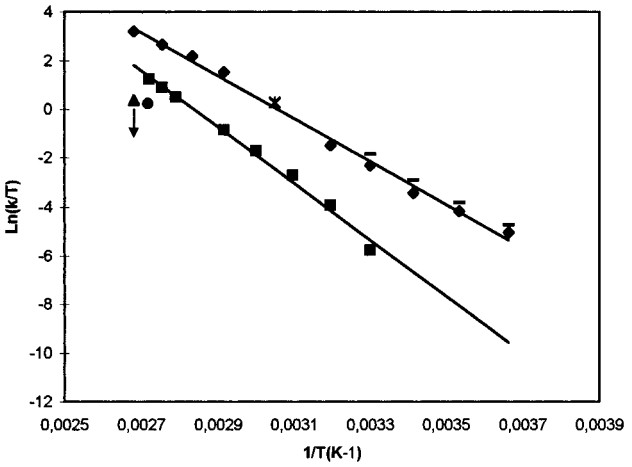

Figure 1. Eyring plot of the *k* values deduced from line shape analysis of the exchanging aminomethyl groups of complexes **8** (■): $\Delta H^{\ddagger} = 96.3$ kJ mol^{-1}, $\Delta S^{\ddagger} = 75.9$ J mol^{-1}. **11M** (◆): $\Delta H^{\ddagger} = 73.5$ kJ mol^{-1}, $\Delta S^{\ddagger} = 27.17$ J mol^{-1}. For complex **11m** (—) this analysis has been carried out only for the slow exchange region below the coalescence temperature (see text) $\Delta H^{\ddagger} = 65.5$ kJ mol^{-1}. The corresponding values calculated from the experimental $\Delta G^{\ddagger}$'s at the coalescence temperatures for complexes **11M** (∗), **13** (●) and **9** (▲) are included.

temperature for complexes **2**−**5** and **7**. Therefore, this general behavior implies that the Pd−N bond rupture in complexes of ligand **1** is a process with a considerably high activation barrier. Similar considerations can be made for PTFA complexes.

In the case of the PPFA complexes, however, a more conclusive analysis of this process can be made. In both Pd(0) and Pd(II) derivatives a general broadening of the aminomethyl resonances is observed while in the case of Pd(PPFA)(DMFU) (**11**),[9d] PdClMe(PPFA) (**8**), and Pd(PPFA)(MA) (**13**), the coalescence temperature is reached. To compare the kinetic parameters of this process, a line shape analysis of the spectra has been carried out for complexes **11** and **8**. The corresponding Eyring plot is depicted in Figure 1, and the kinetic parameters are given in the figure captions. In the case of complex **8** and the major isomer of **11** (**11M**), the analysis was possible over the whole temperature range. However, for **11m** the overlap of lines with those of **11M** has prevented a full analysis in the fast exchange region. A comparison of the data for the two isomers of **11** (see Figure 1) shows some differences. In fact, in the analyzed region, **11M** has lower rate constants as well as higher $\Delta H^{\ddagger}$ values for the bond rupture process. In a previous work[9d] and by means of NOE studies, we have determined the orientation of the DMFU unit in both isomers **11M** and **11m**. In the major isomer the olefin is coordinated with its Re face to the (*S*,*R*)-PPFA palladium unit. An identical arrangement of the DMFU ligand is seen in **2M** (Chart 2), where the olefin also coordinates with its Re side to the (*R*,*R*)-**1** palladium fragment. As compared to **11m**, the steric interaction of the CO_2Me olefin fragment and the ferrocenyl NMe_2 group seems to be less demanding in **11M**, which might be the origin of the higher $\Delta H^{\ddagger}$ observed for the Pd−N bond rupture process in this isomer. If the $\Delta G^{\ddagger}_c$ value for **11M** at the coalescence temperature is used to calculate the rate constant, the resulting value fits perfectly to the straight lines of the Eyring plot (Figure 1).

Table 6. Free Activation Energies Related to the Pd−N Bond Rupture in PPFA Palladium Complexes

entry	complex	$\delta\nu$ (Hz)	T_c (K)	$\Delta G_c^{\ddagger}$ (kJ/mol)
1	Pd(PPFA)(DMFU), **11**		368	63.5[a]
2	**11**		373	63.4[a]
3	PdClMe(PPFA), **8**		368	68.4[a]
4	**8**		373	68.0[a]
5	Pd(PPFA)(MA), **13**	235.3	368	71.6[b]
6	$PdCl_2$(PPFA), **9**	249	>373	>72.4[b]

[a] The $\Delta G_c^{\ddagger}$ has been calculated from a band-shape analysis. [b] See Experimental Section for the calculation method used.

To compare kinetic parameters of the Pd−N bond rupture processes in Pd(0) and Pd(II) complexes, a line shape analysis for complex **8** has also been carried out. The kinetic data are given in Figure 1. In this figure, a *k* value for the complex Pd(PPFA)(MA), **13**, was also added, which was calculated from $\Delta G^{\ddagger}_c$ at the coalescence temperature. A complete line shape analysis for this derivative has not been possible due to overlapping lines and because the line width is also affected by the alkene rotation process. For $PdCl_2$(PPFA), **9**, at 373 K a very pronounced broadening of the aminomethyl signals is observed, but a decomposition process prevents a full variable-temperature NMR study. Hence, only limiting data are given: at 373 K, the *k* value is lower than 550 s^{-1}, which correspond to $\Delta G^{\ddagger}_{373} > 72.4$ kJ mol^{-1}. To make proper comparisons, we have collected in Table 6 the $\Delta G^{\ddagger}_c$ values at 368 or 373 K for the described PPFA complexes **8**, **11**, **13**, and **9**. Although not extremely big, the differences in $\Delta G^{\ddagger}_c$ are significant. If we compare the data at 373 K for complexes **11**, **8**, and **9** (entries 2, 4, and 6), it is clear that the palladium(II) complexes exhibit higher barriers than the palladium(0) derivatives. This may be a consequence of the lower electronic density at the metal in the higher oxidation state. The lower value obtained for complex **8** as compared to **9** may be explained on the basis of the high trans influence of the methyl group that weakens the Pd−N bond. In the comparison of the data at 368 K (entries 1, 3, and 5), the DMFU derivative also shows the lowest value. The substantially higher value of complex **13** as compared to the other palladium(0) derivative, **11**, is likely to be due to the previously stated higher electron withdrawing ability of MA, which makes the metal center a better electron acceptor, thus strengthening the Pd−N bond.

X-ray structure of (1)Pd(MA) (3). Racemic complex **3** crystallizes in the triclinic space group $P\bar{1}$ with two molecules in the asymmetric unit and four molecules in the unit cell. It was with surprise that the two independent molecules of the asymmetric unit are those that in solution were assigned to the minor **3m** and the major diastereomer **3M** with the maleic anhydride unit either pointing away or toward the ferrocenyl core.

A list of selected bond lengths and bond angles is given in Table 7, and experimental parameters for the structure determinations are given in Table 8. An ORTEP of the exo diastereomer is shown in Figure 2.

The general structural features of the ferrocenyl units of both molecules are similar to those found for ligand **1** and its $PdCl_2$ complex. Bond lengths and bond angles are within the usual range, e.g., with average Fe−C_{ar}

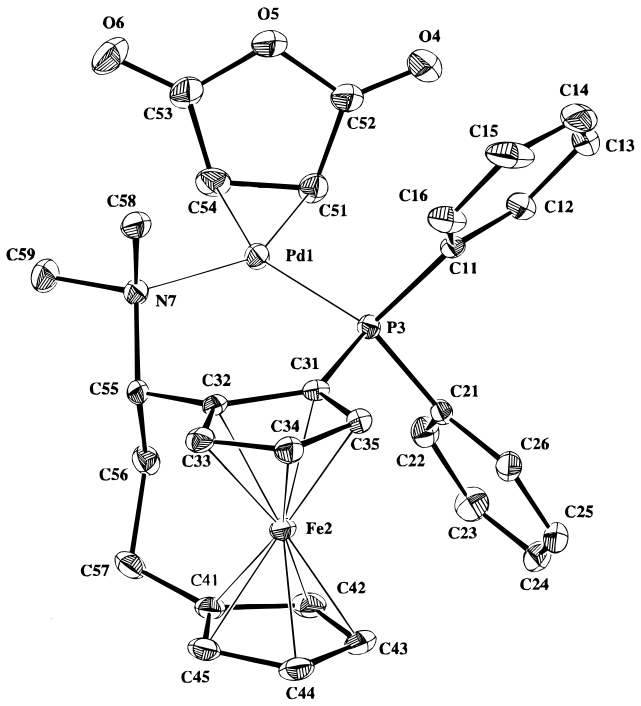

Figure 2. ORTEP drawing of the *exo*-(R,R)-Pd(**1**)(MA) diastereomer of complex **3**.

Table 7. Selected Bond Lengths (Å) and Angles (deg) for 3

Bond Distances			
Pd(1)−C(51)	2.103(5)	Pd(11)−C(511)	2.102(5)
Pd(1)−C(54)	2.128(5)	Pd(11)−C(541)	2.131(5)
Pd(1)−N(7)	2.196(4)	Pd(11)−N(71)	2.201(4)
Pd(1)−P(3)	2.2915(13)	Pd(11)−P(31)	2.306(2)
P(3)−C(31)	1.807(5)	P(31)−C(311)	1.804(5)
N(7)−C(55)	1.514(6)	N(71)−C(551)	1.506(7)
O(4)−C(52)	1.196(7)	O(41)−C(521)	1.206(6)
O(5)−C(52)	1.400(7)	O(51)−C(521)	1.403(6)
O(5)−C(53)	1.410(8)	O(51)−C(531)	1.403(7)
O(6)−C(53)	1.210(8)	O(61)−C(531)	1.201(6)
Bond Angles			
C(51)−Pd(1)−C(54)	39.1(2)	C(511)−Pd(11)−C(541)	39.0(2)
N(7)−Pd(1)−P(3)	95.68(11)	N(71)−Pd(11)−P(31)	96.45(12)
C(54)−Pd(1)−N(7)	111.8(2)	C(541)−Pd(11)−N(71)	109.3(2)
C(51)−Pd(1)−P(3)	113.5(2)	C(511)−Pd(11)−P(31)	115.0(2)
C(31)−P(3)−Pd(1)	111.4(2)	C(311)−P(31)−Pd(11)	110.3(2)
C(55)−N(7)−Pd(1)	113.3(3)	C(551)−N(71)−Pd(11)	111.7(3)
C(32)−C(55)−N(7)	110.9(4)	C(321)−C(551)−N(71)	110.6(4)
C(32)−C(55)−C(56)	113.5(4)	C(321)−C(551)−C(561)	113.9(5)
N(7)−C(55)−C(56)	109.9(4)	N(71)−C(551)−C(561)	110.3(4)
C(55)−C(56)−C(57)	114.6(4)	C(551)−C(561)−C(571)	115.3(5)
C(41)−C(57)−C(56)	114.1(4)	C(411)−C(571)−C(561)	113.8(5)

and $C_{ar}-C_{ar}$ bond lengths of 2.032(8) and 1.42(1) Å (**3m**) and 2.03(1) and 1.42(1) Å (**3M**). The Cp rings are essentially planar. However, the trimethylene bridge forces the Cp rings to be tilted by 8.8° and 10.6°, respectively. In addition, the benzylic bridge carbons are moved out of plane, both toward the inner bridge carbons (C56 and C561). Carbons C55 and C551 are displaced by 0.13 and 0.12 Å below Cp^1 (Cp^1 formed by the following: **3m**, C31−C35; **3M**, C311−C351), while C57 and C571 are out of the plane of Cp^2 (Cp^2 formed by the following: **3m**, C41−C45; **3M**, C411−C451) by 0.18 and 0.12 Å, respectively. Like in the free ligand, the trimethylene bridge adopts a conformation in which the carbon nitrogen bonds (C55−N7 and C551−N71) are positioned almost perpendicular to the respective Cp^1 planes. A comparison with the molecular structure of 1 shows that the formation of a palladium P−N chelate ring imposes conformational changes mostly in the diphenyl phosphine part. One phenyl ring is positioned in close proximity to the Cp^2 protons H42 and H421 (attached to carbons C42 and C421), a fact that in the NMR spectra is reflected by a strong high-field shift of these particular nuclei. At the same time the phosphorus atoms P3 and P31 are severely forced out of plane by 0.30 Å (**3m**) and 0.26 Å (**3M**) above Cp^1.

A superposition (Figure 3) of the molecular structures of **3m** and **3M** shows that the ferrocenyl aminophosphine ligands adopt quite similar conformations in both complexes. Major differences are only seen in the coordination sphere of palladium and in the arrangement of the maleic anhydride unit. In both cases palladium and its coordinated atoms are found in a slightly but differently distorted square planar arrangement. The maleic anhydride ligands are attached to palladium with the Pd−C bonds trans to P being longer than those trans to N, reflecting the stronger trans influence of phosphorus (Pd−C [trans P] 2.128(5) Å (**3m**), 2.130(5) Å (**3M**); Pd−C [trans N] 2.103(5) Å (**3m**), 2.102(5) Å (**3M**)).

The anhydride ligands are essentially planar and bound to the square planar unit with a dihedral angle of 98° (**3m**) and 100° (**3M**), respectively. In **3m** the shortest nonbonding distances of atoms of the maleic

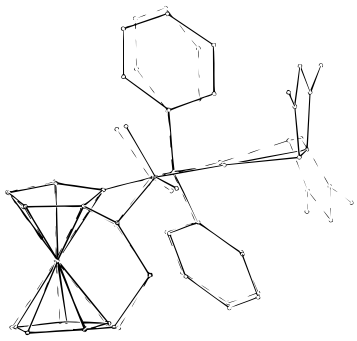

Figure 3. Superposition of the molecular structures of *exo*-(R,R)-Pd(**1**)(MA) (—) and *endo*-(R,R)-Pd(**1**)(MA)(- - -).

Table 8. Crystal Data and Structure Refinement for 3

empirical formula	$C_{62}H_{60}Fe_2N_2O_6P_2Pd_2$
fw	1315.56
temp	293(2) K
wavelength	0.71070 Å
cryst system	triclinic
space group	$P\bar{1}$
unit cell dimensions	$a = 9.8145(7)$ Å; $\alpha = 104.040(10)°$ $b = 13.827(2)$ Å; $\beta = 97.994(7)°$ $c = 21.461(4)$ Å; $\gamma = 102.005(8)°$
volume	2707.9(7) Å^3
Z	2
density (calcd)	1.613 g/cm^3
abs coeff	12.93 cm^{-1}
$F(000)$	1336
crystal size	0.5 × 0.3 × 0.25 mm
θ range for data collection	2.08−20.02°
index ranges	$-9 \le h \le 9$, $-13 \le k \le 13$, $-20 \le l \le 20$
no. of reflections collected	10 130
refinement method	full-matrix least-squares on F^2
no. of data/restraints/parameters	5066/0/685
goodness-of-fit on F^2	1.120
final R indices [$I > 2\sigma(I)$]	R1 = 0.0300, wR2 = 0.0673
R indices (all data)	R1 = 0.0385, wR2 = 0.0736
largest diff peak and hole	0.677 and −0.417 e Å^{-3}

anhydride units to the ferrocenyl core are those of the olefin protons H51 to ortho-Ph_{down} proton H22 (2.32 Å) and H54 to Me_{down} protons H59A and H59B (2.89 and 2.96 Å) and of oxygens O4 to the ortho-Ph_{up} proton H12 (3.04 Å) and O6 with proton H59B (2.75 Å). In **3M** the shortest related distances are those of oxygens O41 to ortho-Ph_{down} H221 (2.55 Å) and O61 to Me_{down} protons H59D and H59F (2.82 and 3.10 Å) and of the olefinic proton H541 to Me_{up} H58E (3.28 Å) and to Me_{down} H59F (2.65 Å). A comparison of these distances in **3m** and **3M** shows that only in **3M** is the olefinic proton H541 (trans P) close enough to the respective Me_{up} group to allow for NOE enhancement as described in the Stereochemical Assignments section. In **3m** the closest distance of H54 (trans P) to a Me_{up} proton is 4.30 Å, much longer than that in **3M** (H541/H59F: 2.65 Å), an argument that has been used in the assignment of **3M** in solution. Intramolecular nonbonding H−H distances have been derived from calculated hydrogen positions.

Conclusions

Several new palladium(0) and -(II) derivatives of ligand **1** and PPFA have been prepared. NMR variable-temperature studies on these complexes have allowed the determination of the activation barriers of different fluxional processes such as alkene rotation, alkene face exchange, apparent allyl rotation, and Pd−N bond rupture. The calculated $\Delta G^{\ddagger}_c$, together with our previously reported data for PPFA and PTFA complexes, allows us to draw the following conclusions: The activation barriers for alkene rotations in the palladium(0) complexes are in the order of **1** > PTFA > PPFA and MA > DMFU. For the DMFU complexes the observed isomerization must imply an alkene face exchange, which according to our results most likely takes place via a dissociative pathway. An apparent allyl rotation is observed for the allyl complexes with the activation barriers following the order **1** > PPFA > PTFA. In Pd(0) and Pd(II) complexes with PPFA, the Pd−N bond rupture is a process with an activation barrier low enough to be observable on the NMR time scale. For derivatives with PTFA or **1**, this process, although feasible, must be of higher energy. The activation barriers are higher in palladium(II) than in palladium(0) complexes, but the donor or acceptor ability of the ancillary ligands is an important factor to be considered. The fact that on the NMR time scale Pd−N bond rupture in complexes with PPFA type aminophosphine ligands is a fast process indicates that the Pd−N bond cleavage may be involved in important steps of different catalytic processes not only in cross-coupling reactions but also in allylic alkylations, allylic aminations, or other similar processes.

Experimental Section

General Comments. All manipulations were carried out under an atmosphere of dry oxygen-free nitrogen using standard Schlenk techniques. Solvents were distilled from the appropriate drying agents and degassed before use. Elemental analyses were performed with a Perkin-Elmer 2400 microanalyzer. IR spectra were recorded as KBr pellets or Nujol mulls with a Perkin-Elmer PE 883 IR spectrometer. ^{1}H, ^{13}C, ^{19}F, and ^{31}P NMR spectra were recorded on a Varian Unity 300 spectrometer. Chemical shifts (ppm) are relative to TMS (^{1}H, ^{13}C NMR), $CClF_3$ (^{19}F NMR), and 85% H_3PO_4 (^{31}P NMR). Coupling constants (J) are in hertz. The NOE difference spectra were recorded with 5000 Hz, acquisition time 3.27 s, pulse width 90°, relaxation delay 4 s, irradiation power 5−10 dB. For variable-temperature spectra, the probe temperature (±1 K) was controlled by a standard unit calibrated with a methanol reference. Free energies of activation were calculated from the coalescence temperature (T_c), and the frequency difference between the coalescing signals (extrapolated at the coalescence temperature) with the formula[28] $\Delta G^{\ddagger}_c = aT(10.319 + \log T/k)$, k values were calculated according to the Shanan-Atidi and Bar-Eli method.[28] In cases of equal populated species (for example, interchange of olefin substituents in **2** or aminomethyl interchange in complexes of Table 6), the formula[28] $\Delta G^{\ddagger}_c = aT(9.972 + \log T/\delta\nu)$ has been used. For the AB system of complex **2** (entry 1 of Table 4), $\Delta G^{\ddagger}_c$ has been calculated from the following expression: $\Delta G^{\ddagger}_c = aT[9.972 + \log(T/(\delta\nu^2 + 6J_{AB}^2)^{1/2})$ ($a = 1.914 \times 10^{-2}$, $\Delta G^{\ddagger}_c$ in kJ mol^{-1}). The estimated error in the calculated free energies of activation is 1.0−1.1 kJ mol^{-1}. $Pd_2(dba)_3$·$CHCl_3$,[29] $[Pd(\eta^3\text{-2-Me-}C_3H_4)Cl]_2$,[30] PdClMe(COD),[31] $Pd(C_6F_5)_2$(COD),[32] and $PdMe_2$(TMEDA)[33] were prepared according to literature methods. DMFU-d_6 was prepared from fumaryl chloride and CD_3OD.

Preparation of Pd(1)(DMFU)·1/4PhCH$_3$ (2·1/4PhCH$_3$). To a degassed solution of $Pd_2(dba)_3$·$CHCl_3$ (90 mg, 0.087 mmol) in 20 mL of toluene are added 87.0 mg (0.191 mmol) of **1** and 36.4 mg (0.252 mmol) of dimethyl fumarate. The solution is stirred for 2 h, filtered, and evaporated to dryness. Free dba is removed from the mixture by chromatography on a Silica 60 column (25 × 1 cm) with toluene as eluent. Complex **2** is eluted with THF and the solution evaporated to dryness. **2·1/4PhCH$_3$** is obtained as an orange solid. Crystals of pure **2M** were obtained by recrystallization from toluene/diethyl ether. Yield: 62.4 mg (0.089 mmol, 51%). Anal. Calcd for $C_{33}H_{36}FeNO_4PPd$·$1/4C_7H_8$: C, 57.42; H, 5.26; N, 1.93. Found: C, 57.59; H, 4.94; N, 1.68. IR: ν(C=O) 1676 cm^{-1}, π(C−H) 882 cm^{-1}. ^{31}P NMR (toluene-d_8): **2M**, 15.83, s; **2m**, 15.44, s.

Preparation of Pd(1)(MA) (3). The procedure is identical to that described for **2**. Amounts are as follows: $Pd_2(dba)_3$·$CHCl_3$ (93.1 mg, 0.090 mmol); **1** (90.0 mg, 0.199 mmol); maleic anhydride (25.7 mg, 0.262 mmol). **3** is obtained as an orange solid. Yield: 40.2 mg (0.061 mmol, 34%). Orange crystals were obtained by vapor diffusion from methylene chloride/diethyl ether. Anal. Calcd for $C_{31}H_{30}FeNO_3PPd$: C, 56.60; H, 4.60; N, 2.12. Found: C, 56.65; H, 4.98; N, 2.09. IR: ν(C=O) 1786, 1717 cm^{-1}; π(C−H) 779 cm^{-1}. ^{31}P NMR (chloroform-d): **3M**, 15.89, s; **3m**, 17.63, s.

Preparation of [Pd(η^3-2-Me-C$_3$H$_4$)(1)]Tf·1/2Et$_2$O (4·1/2Et$_2$O). This complex is prepared in a way similar to that described by Pregosin.[10] To a degassed solution of 35.0 mg (0.089 mmol) of $[Pd(\eta^3\text{-2-Me-}C_3H_4)Cl]_2$ and 80.8 mg of **1** (0.180 mmol) in 20 mL of acetone is added a solution of $AgCF_3SO_3$ (45.7 mg, 0.180 mmol) in 2 mL of methanol. After stirring for 3 h in the dark, the orange solution is filtered over a plug of Celite and evaporated to dryness. The gummy residue is triturated with hexane and diethyl ether, giving **4**·1/2Et_2O as an orange solid. Yield: 71.1 mg (0.116 mmol, 65%). Anal. Calcd for $C_{32}H_{35}F_3FeNO_3PPdS$·$1/2C_4H_{10}O$: C, 50.98; H, 5.03;

(28) Sandström, J. *Dynamic NMR Spectroscopy*; Academic Press: London, 1982.
(29) Ukai, T.; Kawazura, H.; Ishii, Y.; Bonnet, J. J.; Ibers, J. A. *J. Organomet. Chem.* **1974**, *65*, 253.
(30) Dent, W. T.; Wilkinson, A. J. *J. Chem. Soc.* **1964**, 1585.
(31) Rülke, R. E.; Ernsting, J. M.; Spek, A. L.; Elsevier: C. J.; van Leeuwen, P. W. N. M.; Vrieze, K. *Inorg. Chem.* **1993**, *32*, 5769.
(32) Espinet, P.; Martínez-Ilarduya, J. M.; Pérez-Briso, C.; Casado A. L.; Alonso, M. A. *J. Organomet. Chem.* **1998**, *551*, 9.
(33) de Graaf, W.; Boersma, J.; Smeets, W. J. J.; Spek, A. L.; van Koten, G. *Organometallics* **1989**, *8*, 2907.

N,1.75. Found: C, 51.16; H, 4.57; N, 1.79. IR:[34] CF_3SO_3 1271, 1223, 1147, and 636 cm^{-1}; 2-Me-C_3H_4 1029, 1480, 1469, 1435, 829, 839 cm^{-1}. ^{31}P NMR (1,1,2,2,-tetrachloroethane-d_2): **4M**, 16.50, s; **4m**, 19.58, s.

Preparation of PdClMe(1) (5). A degassed solution of 35.1 mg of PdClMe(COD) (0.132 mmol) and 60 mg of **1** (0.132 mmol) in 30 mL of methylene chloride is stirred for 24 h. The reaction mixture is evaporated to dryness, and the gummy residue is washed and triturated with hexane. **5** is obtained as a yellow solid. Yield: 62.0 mg (0.10 mmol, 77%). Anal. Calcd for $C_{28}H_{31}ClFeNPPd$: C, 55.11; H, 5.12; N, 2.29. Found: C, 55.02; H, 4.61; N, 2.82. IR:[34b] ν(Pd−CH_3) 512 cm^{-1}; ν(Pd−Cl) 269 cm^{-1}. ^1H NMR (chloroform-*d*): 0.54 (d), J_{H-P} = 3.7 Hz, Me; ^{13}C NMR (chloroform-*d*): 2.21 (d), J_{C-P} = 8.50 Hz, Me. ^{31}P NMR (chloroform-*d*): 22.97, s.

Preparation of $PdMe_2$(1) (6). A degassed solution of 27.9 mg of $PdMe_2$(TMDA) (0.11 mmol) and 50 mg of **1** (0.11 mmol) in 20 mL of toluene is stirred for 18 h. The pale yellow solution is concentrated up to 3 mL, and 10 mL of hexane are added. **6** is obtained as pale yellow crystals after keeping the solution in a freezer for several hours. Yield: 44.1 mg (0.075 mmol, 68%). Anal. Calcd for $C_{29}H_{34}FeNPPd$: C, 59.05; H, 5.81; N,2.37. Found: C, 59.15; H, 5.81; N, 2.35. IR:[34b] ν(Pd−Me) 523, 510 cm^{-1}. ^1H NMR (benzene-d_6): 0.77 (d), J_{H-Pcis} = 6.8 Hz, Me cis P; 0.83 (d), $J_{H-Ptrans}$ = 8.8 Hz, Me trans P. ^{13}C NMR (benzene-d_6): 5.61 (d), J_{C-Pcis} = 8.50 Hz, Me cis P; 10.10 (d), $J_{C-Ptrans}$ = 114.8 Hz, Me trans P. ^{31}P NMR (benzene-d_6): 6.75, s.

Preparation of $Pd(C_6F_5)_2$(1)·1/2Et_2O (7·1/2Et_2O). A degassed solution of 80.0 mg of **1** (0.180 mmol) and 96.0 mg of $Pd(C_6F_5)_2$(COD) (0.180 mmol) in methylene chloride is refluxed at 40 °C for 2 h. The solvent of the resulting solution is reduced to 3 mL, and a pale yellow precipitate of **7** is formed when diethyl ether is added. Yield: 93.3 mg (0.104 mmol, 58%). Anal. Calcd for $C_{39}H_{28}F_{10}FeNPPd$·1/2$C_4H_{10}O$: C, 52.89; H, 3.57; N, 1.50. Found: C, 53.03; H, 3.14; N, 1.52. IR:[35] C_6F_5 1497, 957, and 789 cm^{-1}. ^{31}P NMR (bencene-d_6): 7.99, s. ^{19}F NMR[36] (benzene-d_6): −114.77, −115.64, −116.46, −117.07 (m, ortho); −163.05, −163.65, −164.14, −164.79 (m, meta); −160.91 (dd, J_{FF} = 21.4, 18.3 Hz, para), −162.24 (dd, J_{FF} = 21.4, 18.3 Hz, para).

Preparation of PdClMe(PPFA) (8). A degassed solution of 36.2 mg of PdClMe(COD) (0.136 mmol) and 60 mg of PPFA (0.136 mmol) in 20 mL of toluene is stirred for 16 h at room temperature. The solution is evaporated to dryness, and the residue is washed and triturated with hexane. A filtration yields **8** as a pale orange solid. Yield: 47 mg (0.079 mmol, 58%). Anal. Calcd for $C_{27}H_{30}ClFeNPPd$: C, 54.30; H, 5.06; N, 2.34. Found: C, 54.08; H, 4.64; N, 2.32. IR:[34b] ν(Pd−CH_3) 501 cm^{-1}, ν(Pd−Cl) 275 cm^{-1}. ^1H NMR (toluene-d_8): 1.12 (d), J_{H-P} = 4.4 Hz, Me. ^{13}C NMR (toluene-d_8): 1.61 (d), J_{C-P} = 3.5 Hz, Me. ^{31}P NMR (toluene-d_8): 24.09, s.

X-ray Structural Analysis of Complex 3. A crystal of approximate dimensions of 0.5 × 0.30 × 0.25 mm was mounted on a glass capillary. Intensity data were collected on a PHILIPS PW1100 diffractometer equipped with graphite Mo Kα radiation (λ = 0.710 73 Å) using an $\omega/2\theta$ scan to a maximum value of 30°. Data were corrected for Lorentz and polarization effects, and absorption correction was not required because the variation in integrated Ψ scan intensities was <10%.

The structure was solved using direct methods (SIR92).[37] Refinement on F^2 was carried out by full-matrix least-squares techniques (SHELXL-93).[38] All non-hydrogen atoms were refined with anisotropic thermal parameters. The hydrogen atoms were included in calculated positions. Refinement converged at the following reliability values: R1 = 0.0300, wR2 = 0.0692 for reflections with $I > 2\sigma I$ and R1 = 0.0385, wR2 = 0.0760 for all reflections. Goodnes-of-fit = 1.12. Maximum and minimum electron density in the final electron density map was 0.677 (near the Pd atom) and −0.417 e $Å^{-3}$.

Acknowledgment. We gratefully acknowledge the Dirección General de Investigación Científica y Técnica (DGICYT, Grant PB95-0901, and Acción Integrada Project HU94-009, Ciudad Real, Spain), the Fonds zur Förderung der Wissenschaftlichen Forschung (Project P09859-CHE), and Österreichischer Akademischer Austauschdienst (ÖAD, Acción Integrada Project 29/95, Wien, Austria).

Supporting Information Available: Crystal data and structure refinement. Tables of positional and atomic displacement parameters for all atoms, anisotropic displacement parameters, bond lengths and bond angles, least-squares planes, important intermolecular contacts, and unit cell and packing diagram of complex **3**. Full ^1H and ^{13}C NMR data for the new complexes (25 pages). Ordering information is given on any current masthead page.

OM980312Z

(34) (a) Shobatake, K.; Nakamoto, K. *J. Am. Chem. Soc.* **1970**, *92*, 2. 3339. (b) Nakamoto, K., Ed. *Infrared and Raman Spectra of Inorganic and Coordination Compounds;* J. Wiley and Sons: New York, 1986.

(35) Deacon, G. B.; Green, J. H. S. *Spectrochim. Acta, Part A* **1968**, *24*, 1125.

(36) Usón, R.; Forniés, J. *Adv. Organomet. Chem.* **1988**, *28*, 219.

(37) Altomare, A.; Cascarano, G.; Giacovazzo, C.; Guagliardi, A.; Burla, M. C.; Polidori, G.; Camalli, M. *J. Appl. Crystallogr.* **1994**, 435.

(38) Sheldrick, G. M. *Program for the Refinement of Structures from Diffraction Data*; University of Göttingen, Göttingen, Germany, 1993.